

# Quantitative Profiling of Protein O-GlcNAcylation Sites by an Isotope-Tagged Cleavable Linker

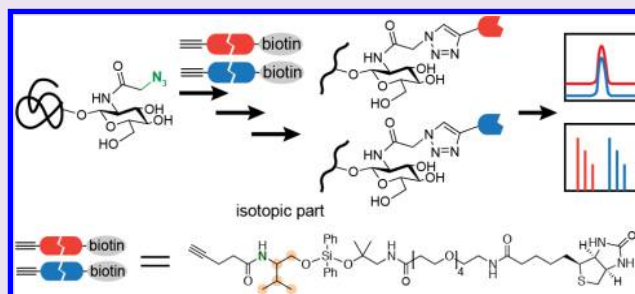
Ke Qin,<sup>†,‡,∇</sup> Yuntao Zhu,<sup>†,‡,∇</sup> Wei Qin,<sup>†,§</sup> Jinjun Gao,<sup>†,§</sup> Xuan Shao,<sup>#</sup> Yan-ling Wang,<sup>#</sup> Wen Zhou,<sup>\*,†,‡</sup> Chu Wang,<sup>\*,†,‡,§,||,⊥</sup> and Xing Chen<sup>\*,†,‡,§,||,⊥</sup>

<sup>†</sup>College of Chemistry and Molecular Engineering, <sup>‡</sup>Beijing National Laboratory for Molecular Sciences, <sup>§</sup>Peking–Tsinghua Center for Life Sciences, <sup>||</sup>Synthetic and Functional Biomolecules Center, and <sup>⊥</sup>Key Laboratory of Bioorganic Chemistry and Molecular Engineering of Ministry of Education, Peking University, Beijing 100871, China

<sup>#</sup>State Key Laboratory of Stem Cells and Reproductive Biology, Institute of Zoology, Chinese Academy of Sciences, Beijing, 100101, China

## Supporting Information

**ABSTRACT:** Large-scale quantification of protein O-linked  $\beta$ -N-acetylglucosamine (O-GlcNAc) modification in a site-specific manner remains a key challenge in studying O-GlcNAc biology. Herein, we developed an isotope-tagged cleavable linker (isoTCL) strategy, which enabled isotopic labeling of O-GlcNAc through bioorthogonal conjugation of affinity tags. We demonstrated the application of the isoTCL in mapping and quantification of O-GlcNAcylation sites in HeLa cells. Furthermore, we investigated the O-GlcNAcylation sensitivity to the sugar donor by quantifying the levels of modification under different concentrations of the O-GlcNAc labeling probe in a site-specific manner. In addition, we applied isoTCL to compare the O-GlcNAcylation stoichiometry levels of more than 100 modification sites between placenta samples from male and female mice and confirmed site-specifically that female placenta has a higher O-GlcNAcylation than its male counterpart. The isoTCL platform provides a powerful tool for quantitative profiling of O-GlcNAc modification.



The O-linked  $\beta$ -N-acetylglucosamine (O-GlcNAc) modification on the serine and threonine residues is a ubiquitous protein glycosylation that occurs intracellularly.<sup>1</sup> More than a thousand of cytosolic, nuclear, and mitochondrial proteins are reported to be O-GlcNAcylated, which play important roles in various biological processes, such as stress response, transcription regulation, and signal transduction.<sup>2–4</sup> O-GlcNAc is dynamically regulated by a pair of enzymes—O-GlcNAc transferase (OGT) and O-GlcNAcase (OGA)—for installing and removing O-GlcNAc, respectively.<sup>5–7</sup> Aberrant regulation of O-GlcNAc homeostasis has been implicated in various diseases, including diabetes, cancers, and neurological disorders.<sup>4,8–10</sup> Selective enrichment and proteomic identification of O-GlcNAcylated proteins have greatly advanced our understanding of O-GlcNAc biology and pathology.<sup>3</sup> However, site-specific mapping and quantification of O-GlcNAc modification at the proteome level remains challenging, mainly because O-GlcNAcylation is usually substoichiometric and the glycosidic linkage is highly labile.

To address this challenge, two indispensable technical components must be developed and implemented simultaneously: an efficient method for enrichment of O-GlcNAcylated peptides and a mass spectrometry (MS)-based strategy for large-scale identification and quantification of the modification sites. O-GlcNAc-recognizing lectins and chemical

labeling methods have been developed to enrich O-GlcNAcylated peptides.<sup>11–15</sup> Tandem MS with electron transfer dissociation (ETD) fragmentation can be employed to preserve the labile glycosidic linkage for site identification.<sup>14</sup> In combination with quantitative proteomic techniques such as isotope dimethyl labeling, stable isotope labeling by amino acids in cell culture (SILAC), isobaric tags for relative and absolute quantification (iTRAQ), or label-free quantification, it enables quantitative profiling of modification sites.<sup>16–19</sup> For example, employing chemoenzymatic labeling of O-GlcNAc with azides using a mutant galactosyltransferase (Y289L GalT), which enabled chemoselective reaction with the alkyne-containing affinity tag via copper(I)-catalyzed azide–alkyne cycloaddition (CuAAC or click chemistry),<sup>20</sup> Liu and co-workers recently mapped O-GlcNAcylation sites in the human brain.<sup>18</sup> By integrating iTRAQ, they identified ~1000 O-GlcNAcylation sites, and the abundance of 131 O-GlcNAcylated peptides was found to be altered in Alzheimer's disease (AD) brains.<sup>18</sup> Woo, Bertozzi, and co-workers metabolically labeled O-GlcNAc with azides, and used label-free quantification to investigate O-GlcNAcylation changes

Received: May 5, 2018

Accepted: July 24, 2018

Published: July 30, 2018

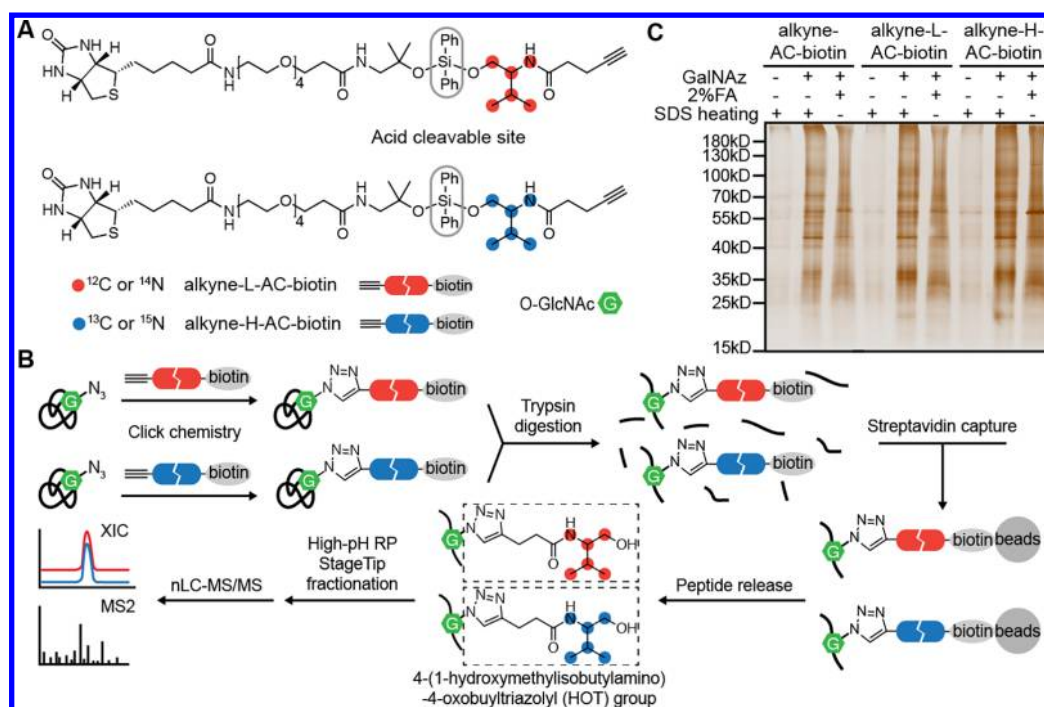


**Figure 1.** isoTCL for quantitative and site-specific profiling of protein O-GlcNAc modification. (A) Structures of alkyne-L-AC-biotin and alkyne-H-AC-biotin. (B) Workflow of isoTCL enrichment and LC-MS/MS analysis of O-GlcNAcylated peptides. (C) Lysates of HeLa cells treated with 200  $\mu$ M GalNAz or vehicle were reacted with alkyne-AC-biotin, alkyne-L-AC-biotin, or alkyne-H-AC-biotin via copper(I)-catalyzed azide–alkyne cycloaddition (CuAAC), followed by incubation with streptavidin beads. The beads were then incubated in 2% formic acid (FA) for 2 h or heated in a 10% SDS loading buffer for 10 min. The released proteins were resolved by SDS-PAGE and stained by silver staining.

during T-cell activation.<sup>19</sup> For mapping the O-GlcNAc sites, they employed Isotope Targeted Glycoproteomics (IsoTaG), a method developed by the same group, which installed an isotopic tag onto O-GlcNAc as a mass-independent signature for improving the selection and identification of glycopeptides in MS.<sup>21–24</sup>

Herein, we report an O-GlcNAc identification and quantification method based on an isotope-tagged cleavable linker (isoTCL) strategy, which introduces isotopic labeling of O-GlcNAc through bioorthogonal conjugation of affinity tags (see Figure 1). The isoTCL method was inspired by the isotopic tandem orthogonal proteolysis–activity-based protein profiling (isoTOP-ABPP) strategy, which labels specific protein residues in an activity-dependent manner with chemical probe affinity tags, followed by conjugation with isotopically labeled affinity tags for proteomic quantification.<sup>25–28</sup> To quantify O-GlcNAcylation, we designed and synthesized a pair of alkyne-biotin tags containing an acid-cleavable dialkoxydiphenylsilane (DADPS) linker<sup>29</sup> that are isotopically labeled, respectively (“light” alkyne-L-AC-biotin and “heavy” alkyne-H-AC-biotin; see Figure 1A). The O-GlcNAc proteins can be metabolically or chemoenzymatically labeled with azides, followed by reaction with alkyne-L-AC-biotin and alkyne-H-AC-biotin and enrichment with streptavidin beads. After cleavage of DADPS by acid, a “heavy” 4-(1-hydroxymethylisobutylamino)-4-oxobutyltriazolyl (HOT) group with five <sup>13</sup>C and one <sup>15</sup>N or a “light” counterpart with a molecular weight difference of 6.0138 Da remains on the O-GlcNAc moiety (Figure 1B). ETD-based tandem mass spectroscopy (MS) is then used to quantify the modification sites by comparing the light/heavy ratios (Figure 1B). Comparing to the previous methods, in which quantification at the peptide level were used for O-GlcNAc quantifica-

tion,<sup>16–18</sup> isoTCL installs isotopic tags directly onto the O-GlcNAc moiety for quantification. In addition, the isotopic tags can serve a dual function as a MS1 filter for improving identification confidence by generating a characteristic isotopic pattern.

To synthesize alkyne-L-AC-biotin and alkyne-H-AC-biotin, we used “light” and “heavy” valine to generate the “light” and “heavy” alkynyl alcohol, **5L** and **5H**, respectively (see Scheme S1A in the Supporting Information). A tertiary alcohol-containing biotin, **6**, was synthesized as previously reported,<sup>29</sup> which was first reacted with excess dichlorodiphenylsilane and then with **5L** or **5H** to afford alkyne-L-AC-biotin (**7L**) and alkyne-H-AC-biotin (**7H**). An alkyne-AC-biotin (**8**) without the HOT moiety was synthesized as a control (see Scheme S1B in the Supporting Information).

The labeling and cleavage efficiency of the three biotin probes were evaluated by reacting with lysates of HeLa cells treated with 200  $\mu$ M *N*-azidoacetylgalactosamine (GalNAz), which is a chemical reporter for metabolic labeling of O-GlcNAc.<sup>30</sup> Through the GalNAc salvage pathway, GalNAz is metabolized to UDP-GalNAz, which is interconverted with UDP-GlcNAz by UDP-galactose-4-epimerase (GALE). As a result, mucin-type O-linked glycoproteins, N-linked glycoproteins, and O-GlcNAcylated proteins are all metabolically labeled with azides.<sup>19,21,23,30</sup> GalNAz was chosen in order to avoid artificial S-glycosylation induced by per-O-acetylated GalNAz (Ac<sub>4</sub>GalNAz).<sup>31</sup> The biotinylated lysates were captured with streptavidin beads and eluted by a mild acid cleavage (i.e., 2% formic acid) or heating the beads in denaturing SDS loading buffer (see Figure S1A in the Supporting Information). Denaturation ensures the complete release of captured O-GlcNAcylated proteins, but is often contaminated with proteins nonspecifically absorbed by

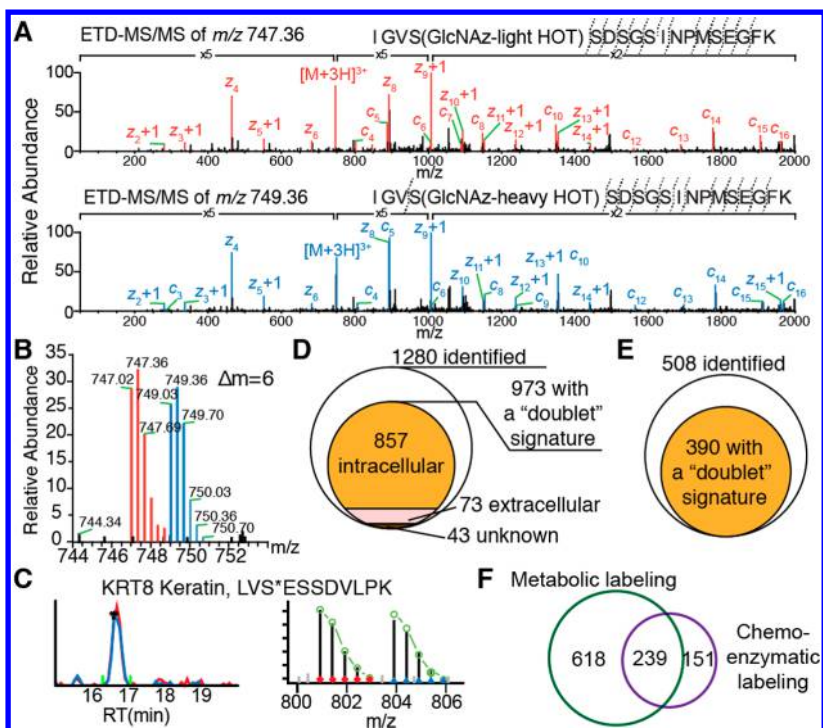


**Figure 2.** Site-specific identification of O-GlcNAc in HeLa cells with isotopic filtering. (A) Representative ETD MS2 spectra of "light" HOT-GlcNAz-peptide and "heavy" HOT-GlcNAz-peptide. An O-GlcNAc peptide from Nup153 is shown. (B) MS1 spectra of the "light" (red lines) and "heavy" (blue lines) ion pair of the HOT-GlcNAz-peptide from Nup153. A mass shift of 6 Da between "light" and "heavy" peptides was observed for the mass envelope, corresponding to the isotopic pattern encoded by isoTCL. (C) Extracted ion chromatogram (XIC) and isotopic envelope of a HOTAz-peptide from KRT8 which is generally marked as a contaminant from sample preparation. (D) Number of identified O-HexNAc sites in GalNAz-treated HeLa cells from three biological replicates. The list was filtered based on the existence of a "doublet" MS1 isotopic envelope. The subcellular location was used to differentiate intracellular O-GlcNAc and cell-surface O-GalNAc modifications. (E) Number of identified O-GlcNAc sites in HeLa cells labeled by the Y289L GalT-based chemoenzymatic method from three biological replicates. (F) Comparison of identified O-GlcNAc sites between metabolic labeling and chemoenzymatic labeling.

streptavidin beads. SDS-PAGE with silver staining demonstrated that all three alkyne-AC-biotin probes reacted with azide-labeled glycoproteins with high efficiency and selectively enriched the labeled proteins with high recovery rate (Figure 1C).

For chemical proteomic analysis, we first attempted a "protein-centric" strategy in which probe-labeled proteins were enriched by streptavidin and subjected to a standard tandem orthogonal proteolysis strategy<sup>32</sup> with on-bead trypsin digestion and acid cleavage to release the modified peptides (see Figure S1A). We first analyzed the released peptides by LC-MS/MS with collision-induced dissociation (CID) fragmentation, which has been reported to break the labile O-GlcNAc glycosidic linkage.<sup>33,34</sup> This resulted in signature ions in the MS2 spectra, including a peptide ion with neutral loss and a series of oxonium ions from the O-GlcNAc moiety, which confirmed the chemical structure of the GlcNAz-modified peptides after bioorthogonal conjugation and acid cleavage (Figure S2 in the Supporting Information). Next, we employed ETD for fragmentation of the modified peptides so that the glycosidic linkage could be preserved and the modification sites could be unambiguously identified (Figure 2A). Notably, the isoTCL encoded a doublet signature (M, M+6) to the mass envelope of any modified peptide in the full MS spectrum, which significantly improves the confidence of O-GlcNAc identification through MS isotopic envelope filtering (Figure 2B, as well as Figure S3 in the Supporting Information). For example, a modification site on keratin 8,

which otherwise would have been excluded as one of the common protein contaminants, was identified with high confidence by the unique isotopic envelope (Figure 2C). Of these two fragmentation methods, CID identified fewer numbers of O-GlcNAcylated peptides, probably because the generation of oxonium ions compromised the efficiency of peptide backbone fragmentation (Figure S4A in the Supporting Information). Assignment of the modification site in this fragmentation mode was further hampered by the low preservation of the O-GlcNAc linkage in MS2 (see Figure S4B in the Supporting Information).

We next optimized the protocol for enrichment of O-GlcNAcylated peptides. By using a peptide-centric enrichment workflow,<sup>35,36</sup> in which in-solution trypsin digestion of the click-labeled protein lysates was performed before capture by streptavidin beads (see Figure S1B in the Supporting Information). We reasoned that the peptide-centric enrichment workflow might reduce nonspecific protein binding on streptavidin beads. Accordingly, an increased number of O-GlcNAcylated sites were identified (Figure S1C in the Supporting Information). In addition, fractionation of the released peptides by high-pH reverse-phase liquid chromatography (RPLC) in a StageTip format<sup>37</sup> before LC-MS/MS analysis resulted in a further increase in the number of identified sites (Figure S1D in the Supporting Information). Therefore, the optimized O-GlcNAc peptide enrichment procedure and ETD-based MS analysis were employed for the following experiments (Figure 1B).

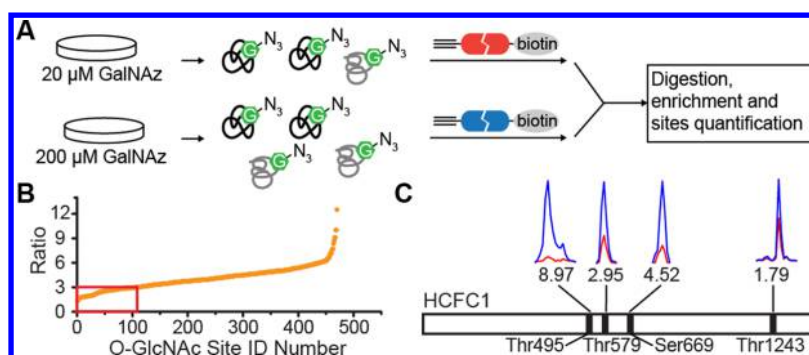


**Figure 3.** Quantifying O-GlcNAcylation propensity site-specifically in proteomes. (A) HeLa cells were treated with 20  $\mu\text{M}$  or 200  $\mu\text{M}$  GalNAz, and the cell lysates were reacted with alkyne-L-AC-biotin and alkyne-H-AC-biotin, respectively. The “light” and “heavy” samples were then mixed, digested, enriched, and analyzed by LC-MS/MS. (B) Distribution of H/L ratios of quantified O-GlcNAc sites; the ratios were calculated from at least two replicates, and hyper-sensitive O-GlcNAc sites whose ratios were  $<3$  appear in the red box. (C) XIC of four representative modification sites on HCFC1; the quantified ratios are shown below each chromatograph.

For mapping the O-GlcNAc sites, the lysates from GalNAz-treated HeLa cells were reacted with the alkyne-L-AC-biotin and alkyne-H-AC-biotin, respectively. After combining the isoTCL-labeled lysates at a 1:1 ratio, the peptides were enriched and analyzed by ETD-MS/MS. A streamlined MS data analysis procedure was established for O-GlcNAc peptide identification and site localization (Figure S3 in the Supporting Information). The distribution of the light/heavy peptide ratios showed a mean of 1.01, accurately matching the premixed isoTCL ratio (see Figure S5A in the Supporting Information). To ensure high confidence of identification, only the O-HexNAc peptides with an isoTCL ratio between 0.67 and 1.5 were selected for site assignment, resulting in a total of 973 O-HexNAc modification sites (Figure 2D and Table S1 in the Supporting Information). Because GalNAz can label both intracellular O-GlcNAc and cell-surface O-glycoproteins, the O-GlcNAc modified peptide can only be differentiated from O-GalNAc (Tn) modified ones having the same molecular weight by subcellular localization.<sup>21</sup> Of the 973 O-HexNAc sites, 857 sites on intracellular proteins including nuclear, cytoplasmic, or mitochondrial proteins were assigned with high-confidence O-GlcNAc sites (see Figure 2D, as well as Figure S5B in the Supporting Information).

The isoTCL strategy is also compatible with the chemoenzymatic labeling method, which uses a mutant galactosyltransferase (Y289L GalT) to transfer a GalNAz onto endogenous O-GlcNAcylation in lysates.<sup>38,39</sup> Using a similar enrichment and data analysis procedure (Figure S6 in the Supporting Information), we identified 390 O-GlcNAcylation sites from HeLa cells (see Figure 2E, as well as Figure S5C and Table S1 in the Supporting Information). In addition, 239 (61%) of these sites were identified in the metabolically labeled samples by GalNAz (Figure 2F). The metabolic labeling reflects the dynamic processes including conversion of GalNAz to UDP-GlcNAz and OGT-catalyzed transfer of GlcNAz onto the newly synthesized O-GlcNAz, thus enabling identification of O-GlcNAcylation sites over time in dynamic states. By comparison, the GalT labeling method allows identification of endogenous O-GlcNAcylation sites in specific cellular states. These results demonstrate the complementarity of the two chemical labeling methods.

A total number of 1008 O-GlcNAcylation sites were identified from HeLa cells by a combination of metabolic glycan labeling and chemoenzymatic labeling. These sites were distributed on 404 proteins (see Figure S7A and Table S2 in

the Supporting Information), which were functionally enriched for protein binding, poly(A) RNA binding, and DNA binding, as shown by Gene Ontology analysis (see Figure S7B in the Supporting Information). While a majority of these proteins ( $>75\%$ ) have fewer than three modification sites identified (Figure S7C in the Supporting Information), some of them were interestingly found to contain a large number of modification sites. For example, 43, 39, and 22 sites were identified for HCFC1, NUP214, and EMSY, respectively (Figure S7D in the Supporting Information). In agreement with our data, many of these proteins were previously reported to have multiple modification sites.<sup>19,40</sup> Sequence analysis around the identified O-GlcNAc sites using pLogo<sup>41</sup> revealed the OGT preferred motifs, P/V–P–T/V–gS–S/T–A/S and P/V–P–T/V–gT–S/T–A/S (Figure S7E in the Supporting Information), which were in agreement with the previous studies.<sup>18</sup>

To verify the accuracy of isoTCL quantification, the GalNAz-incorporated lysates were reacted with alkyne-L-AC-biotin or alkyne-H-AC-biotin, and mixed at varying ratios (1:4, 1:2, 1:1, 2:1, and 4:1). The means of the light/heavy peptide ratios closely matched the expected values (see Figure S8A in the Supporting Information). As shown by the chromatographs of two representative peptides from Nup153 and RBM14, the isoTCL-labeled light/heavy peptides coeluted with characteristic isotopic patterns (see Figure S8B in the Supporting Information).

O-GlcNAcylation is catalyzed by the sole enzyme OGT using UDP-GlcNAc as the sugar donor. However, the mechanism of substrate recognition by OGT is not fully understood.<sup>42–45</sup> Kinetic analysis of hOGT had shown that O-GlcNAcylation levels of substrate proteins did not uniformly respond to changes of the sugar donor,<sup>46</sup> and we therefore proposed that the O-GlcNAcylation sensitivity to the sugar donor could be inherently encoded in a site-specific manner. In combination with metabolic labeling, isoTCL provided a means to quantify the propensity of O-GlcNAcylation for each residue examined by comparing the levels of modification under different concentrations of probe labeling. HeLa cells were treated with GalNAz at low and high concentrations (20  $\mu\text{M}$  and 200  $\mu\text{M}$ ), and the lysates were reacted with alkyne-L-AC-biotin and alkyne-H-AC-biotin, respectively. The proteomes were combined for digestion, enrichment and site-specific quantification (Figure 3A). The sites with lower ratios indicated that the level of O-GlcNAcylation was closer to

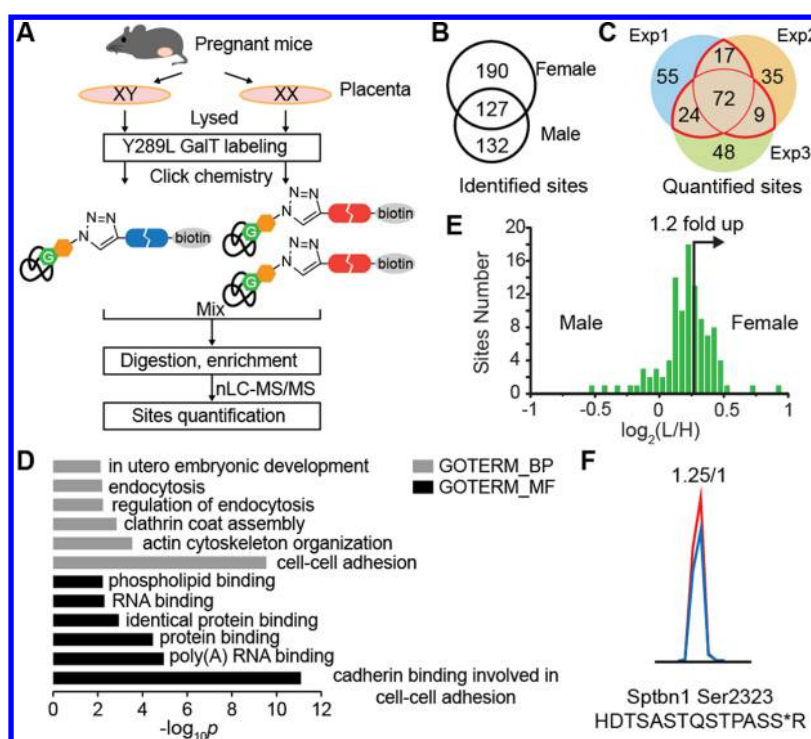


**Figure 4.** Quantitative and site-specific comparison of O-GlcNAcylation between the female and male mouse placentas. (A) The female and male placentas were collected at embryonic day 18.5, lysed, Y289L GalT-labeled, and reacted with alkyne-L-AC-biotin and alkyne-H-AC-biotin, respectively. After mixing the samples at the 1:1 ratio, the lysates were digested, enriched, and analyzed by LC-MS/MS. (B) Overlap of O-GlcNAc sites identified from the female and male placentas. (C) Overlap of quantified O-GlcNAc sites from three biological replicates. The sites quantified from at least two replicates were considered as high-confidence sites (denoted in the bold red circle). (D) GO analysis of O-GlcNAcylated proteins harboring the sites quantified with high-confidence. (E) Distribution of L/H ratios of quantified O-GlcNAc sites. (F) Representative XIC of reported O-GlcNAc sites with up-regulated O-GlcNAcylation from *Sptbn1*.

saturation already at the low concentration of UDP-GlcNAz, suggesting that they are preferred (“hyper-sensitive”) substrate sites modified by OGT. We collectively quantified 470 O-GlcNAc sites from two replicated experiments, and, using  $R < 3$  as the cutoff, ~100 sites were defined as hyper-sensitive O-GlcNAcylated residues (see Figure 3B, as well as Table S3 in the Supporting Information). Our data revealed that the ratios could indeed vary significantly on proteins with multiple modification sites. For example, HCFC1 was quantified with ratios of 8.97, 2.95, 4.52, and 1.79 for Thr495, Thr579, Ser669, and Thr1243, respectively (Figure 3C). The lower ratios of Thr579 and Thr1243 suggested that they were better substrates for OGT and may play key roles in regulating the function of HCFC1.

Finally, we applied isoTCL to quantify O-GlcNAcylation in the mouse placentas. As an X-linked gene, the OGT expression and the overall O-GlcNAc level were found to be lower in male placentas, compared to the female counterpart.<sup>47</sup> OGT was shown to serve as an important placental biomarker of maternal stress and the gender difference in O-GlcNAcylation was proposed to play important roles in sex-biased neurodevelopmental disorders.<sup>47–49</sup> To quantify the site-specific difference of O-GlcNAcylation, we collected placentas from three male and three female mice, respectively, and subjected them to isoTCL analysis. We first confirmed the lower OGT mRNA level in male placentas by qRT-PCR and the lower O-GlcNAcylation level by in-gel fluorescence with Y289L GalT labeling (Figure S9 in the Supporting Information). The female and male placenta lysates were next labeled by Y289L GalT and reacted with alkyne-L-AC-biotin and alkyne-H-AC-

biotin, respectively (Figure 4A). In total, 259 and 317 O-GlcNAcylation sites were identified from the male and female placentas, respectively, with 127 common sites identified in both samples (see Figure 4B, as well as Table S4 in the Supporting Information). Of all these identified O-GlcNAc sites, 105 were quantified from at least two replicates with a standard deviation of  $< 0.3$  (see Figure 4C and Table S4). They are distributed on 76 O-GlcNAcylated proteins, which were significantly enriched in biological processes such as cell–cell adhesion and in utero embryonic development (Figure 4D). Comparing to O-GlcNAc quantification in cell lines, the difference between replicate experiments in the placenta samples was significantly greater. This greater difference was probably due to greater individual differences between living animals, which was also observed in previous studies.<sup>47</sup>

The mean light/heavy ratio of all quantified sites was 1.2, which confirmed that O-GlcNAcylation in the female placenta is, overall, higher (Figure 4E). In total, ~40% O-GlcNAc sites in the female placenta possessed a higher O-GlcNAcylation level by more than 1.2-fold, compared with the males. For example, we found the O-GlcNAc modification on Ser2323 of *Sptbn1*, which had been previously reported as an O-GlcNAc site,<sup>15</sup> was ~1.25-fold higher in the female placentas (Figure 4F). Considering that the dysfunction or deficiency of *Sptbn1* resulted in early embryonic death,<sup>50</sup> we speculated that O-GlcNAcylation on Ser2323 might regulate the function of *Sptbn1* to improve the development of female placentas. These results provide invaluable information for understanding the functional significance of higher O-GlcNAc of the female placenta in maternal stress responses.

In summary, we have designed and synthesized an isotope-tagged cleavable linker for site-specific identification and quantification of protein O-GlcNAcylation. With an optimized sample preparation and ETD-based MS analysis protocol, the isoTCL strategy was applied to profile metabolically labeled or chemoenzymatically labeled O-GlcNAcylated proteomes. We found that the O-GlcNAcylation dynamics responded to the changes of sugar donor concentration site-specifically, with variations observed on different modification sites of the same proteins. Furthermore, isoTCL enabled quantitative comparison of O-GlcNAcylation between the male and female mouse placentas. We envision that isoTCL will find broad applications in quantitative profiling of O-GlcNAcylation. In addition, the isoTCL strategy can be readily applied to other post-translational modifications, such as lipidation and methylation, which can be labeled with azides.<sup>51</sup>

## METHODS

Details of experimental materials and methods are provided in the Supporting Information.

## ASSOCIATED CONTENT

### Supporting Information

The Supporting Information is available free of charge on the ACS Publications website at DOI: 10.1021/acscchembio.8b00414.

Experimental details, compound synthesis, and supporting figures (PDF)

Dataset of all identified O-HexNAc sites (XLSX)

Dataset of identified high-confident O-GlcNAc sites (XLSX)

Dataset of quantified O-GlcNAc sites (XLSX)

Dataset of O-GlcNAc sites in mouse placentas (XLSX)

## AUTHOR INFORMATION

### Corresponding Authors

\*E-mail: wen.zhou@pku.edu.cn (W. Zhou).

\*E-mail: chuawang@pku.edu.cn (C. Wang).

\*E-mail: xingchen@pku.edu.cn (X. Chen).

### ORCID

Jinjun Gao: 0000-0002-7390-5578

Chu Wang: 0000-0002-6925-1268

Xing Chen: 0000-0002-3058-7370

### Author Contributions

<sup>†</sup>These authors contributed equally.

### Notes

The authors declare no competing financial interest.

## ACKNOWLEDGMENTS

This work is supported by National Natural Science Foundation of China (Nos. 91753206, 21425204, and 21521003 to X.C., Nos. 81490740, 21778004, and 21521003 to C.W., and No. 21708002 to W.Z.), and National Key R&D Program of China (No. 2016YFA0501500 to X.C. and C.W., and 2018YFA0507600 to X.C.).

## REFERENCES

(1) Yang, X., and Qian, K. (2017) Protein O-GlcNAcylation: emerging mechanisms and functions. *Nat. Rev. Mol. Cell Biol.* 18, 452–465.

(2) Wells, L., Vosseller, K., and Hart, G. W. (2001) Glycosylation of nucleocytoplasmic proteins: signal transduction and O-GlcNAc. *Science* 291, 2376–2378.

(3) Ma, J., and Hart, G. W. (2014) O-GlcNAc profiling: from proteins to proteomes. *Clin. Proteomics* 11, 8.

(4) Bond, M. R., and Hanover, J. A. (2015) A little sugar goes a long way: The cell biology of O-GlcNAc. *J. Cell Biol.* 208, 869–880.

(5) Haltiwanger, R. S., Holt, G. D., and Hart, G. W. (1990) Enzymatic addition of O-GlcNAc to nuclear and cytoplasmic proteins. Identification of a uridine diphospho-N-acetylglucosamine:peptide beta-N-acetylglucosaminyltransferase. *J. Biol. Chem.* 265, 2563–2568.

(6) Lubas, W. A., Frank, D. W., Krause, M., and Hanover, J. A. (1997) O-Linked GlcNAc transferase is a conserved nucleocytoplasmic protein containing tetratricopeptide repeats. *J. Biol. Chem.* 272, 9316–9324.

(7) Gao, Y., Wells, L., Comer, F. I., Parker, G. J., and Hart, G. W. (2001) Dynamic O-glycosylation of nuclear and cytosolic proteins: cloning and characterization of a neutral, cytosolic beta-N-acetylglucosaminidase from human brain. *J. Biol. Chem.* 276, 9838–9845.

(8) Slawson, C., and Hart, G. W. (2011) O-GlcNAc signalling: implications for cancer cell biology. *Nat. Rev. Cancer* 11, 678–684.

(9) Yuzwa, S. A., and Vocadlo, D. J. (2014) O-GlcNAc and neurodegeneration: biochemical mechanisms and potential roles in Alzheimer's disease and beyond. *Chem. Soc. Rev.* 43, 6839–6858.

(10) Vaidyanathan, K., and Wells, L. (2014) Multiple tissue-specific roles for the O-GlcNAc post-translational modification in the induction of and complications arising from type II diabetes. *J. Biol. Chem.* 289, 34466–34471.

(11) Trinidad, J. C., Barkan, D. T., Gulledge, B. F., Thalhammer, A., Sali, A., Schoepfer, R., and Burlingame, A. L. (2012) Global identification and characterization of both O-GlcNAcylation and phosphorylation at the murine synapse. *Mol. Cell. Proteomics* 11, 215–229.

(12) Alfaro, J. F., Gong, C.-X., Monroe, M. E., Aldrich, J. T., Clauss, T. R. W., Purvine, S. O., Wang, Z., Camp, D. G., Shabanowitz, J., Stanley, P., Hart, G. W., Hunt, D. F., Yang, F., and Smith, R. D. (2012) Tandem mass spectrometry identifies many mouse brain O-GlcNAcylated proteins including EGF domain-specific O-GlcNAc transferase targets. *Proc. Natl. Acad. Sci. U. S. A.* 109, 7280–7285.

(13) Wang, Z., Udeshi, N. D., O'Malley, M., Shabanowitz, J., Hunt, D. F., and Hart, G. W. (2010) Enrichment and site mapping of O-linked N-acetylglucosamine by a combination of chemical/enzymatic tagging, photochemical cleavage, and electron transfer dissociation mass spectrometry. *Mol. Cell. Proteomics* 9, 153–160.

(14) Chalkley, R. J., Thalhammer, A., Schoepfer, R., and Burlingame, A. L. (2009) Identification of protein O-GlcNAcylation sites using electron transfer dissociation mass spectrometry on native peptides. *Proc. Natl. Acad. Sci. U. S. A.* 106, 8894–8899.

(15) Vosseller, K., Trinidad, J. C., Chalkley, R. J., Specht, C. G., Thalhammer, A., Lynn, A. J., Snedecor, J. O., Guan, S., Medzihradsky, K. F., Maltby, D. A., Schoepfer, R., and Burlingame, A. L. (2006) O-linked N-acetylglucosamine proteomics of post-synaptic density preparations using lectin weak affinity chromatography and mass spectrometry. *Mol. Cell. Proteomics* 5, 923–934.

(16) Khidekel, N., Ficarro, S. B., Clark, P. M., Bryan, M. C., Swaney, D. L., Rexach, J. E., Sun, Y. E., Coon, J. J., Peters, E. C., and Hsieh-Wilson, L. C. (2007) Probing the dynamics of O-GlcNAc glycosylation in the brain using quantitative proteomics. *Nat. Chem. Biol.* 3, 339–348.

(17) Myers, S. A., Panning, B., and Burlingame, A. L. (2011) Polycomb repressive complex 2 is necessary for the normal site-specific O-GlcNAc distribution in mouse embryonic stem cells. *Proc. Natl. Acad. Sci. U. S. A.* 108, 9490–9495.

(18) Wang, S., Yang, F., Petyuk, V. A., Shukla, A. K., Monroe, M. E., Gritsenko, M. A., Rodland, K. D., Smith, R. D., Qian, W.-J., Gong, C.-X., and Liu, T. (2017) Quantitative proteomics identifies altered O-GlcNAcylation of structural, synaptic and memory-associated proteins in Alzheimer's disease. *J. Pathol.* 243, 78–88.

- (19) Woo, C. M., Lund, P. J., Huang, A. C., Davis, M. M., Bertozzi, C. R., and Pitteri, S. J. (2018) Mapping and Quantification of Over 2000 O-linked Glycopeptides in Activated Human T Cells with Isotope-Targeted Glycoproteomics (Isotag). *Mol. Cell. Proteomics* 17, 764–775.
- (20) Rostovtsev, V. V., Green, L. G., Fokin, V. V., and Sharpless, K. B. (2002) A stepwise huigen cycloaddition process: copper(I)-catalyzed regioselective “ligation” of azides and terminal alkynes. *Angew. Chem., Int. Ed.* 41, 2596–2599.
- (21) Woo, C. M., Iavarone, A. T., Spiciarich, D. R., Palaniappan, K. K., and Bertozzi, C. R. (2015) Isotope-targeted glycoproteomics (IsoTaG): a mass-independent platform for intact N- and O-glycopeptide discovery and analysis. *Nat. Methods* 12, 561–567.
- (22) Woo, C. M., and Bertozzi, C. R. (2016) Isotope Targeted Glycoproteomics (IsoTaG) to Characterize Intact, Metabolically Labeled Glycopeptides from Complex Proteomes. *Curr. Protoc. Chem. Biol.* 8, 59–82.
- (23) Woo, C. M., Felix, A., Byrd, W. E., Zuegel, D. K., Ishihara, M., Azadi, P., Iavarone, A. T., Pitteri, S. J., and Bertozzi, C. R. (2017) Development of IsoTaG, a Chemical Glycoproteomics Technique for Profiling Intact N- and O-Glycopeptides from Whole Cell Proteomes. *J. Proteome Res.* 16, 1706–1718.
- (24) Woo, C. M., Felix, A., Zhang, L., Elias, J. E., and Bertozzi, C. R. (2017) Isotope-targeted glycoproteomics (IsoTaG) analysis of sialylated N- and O-glycopeptides on an Orbitrap Fusion Tribrid using azido and alkynyl sugars. *Anal. Bioanal. Chem.* 409, 579–588.
- (25) Weerapana, E., Wang, C., Simon, G. M., Richter, F., Khare, S., Dillon, M. B. D., Bachovchin, D. A., Mowen, K., Baker, D., and Cravatt, B. F. (2010) Quantitative reactivity profiling predicts functional cysteines in proteomes. *Nature* 468, 790–795.
- (26) Qian, Y., Martell, J., Pace, N. J., Ballard, T. E., Johnson, D. S., and Weerapana, E. (2013) An Isotopically Tagged Azobenzene-Based Cleavable Linker for Quantitative Proteomics. *ChemBioChem* 14, 1410–1414.
- (27) Wang, C., Weerapana, E., Blewett, M. M., and Cravatt, B. F. (2014) A chemoproteomic platform to quantitatively map targets of lipid-derived electrophiles. *Nat. Methods* 11, 79–85.
- (28) Yang, J., Tallman, K. A., Porter, N. A., and Liebler, D. C. (2015) Quantitative chemoproteomics for site-specific analysis of protein alkylation by 4-hydroxy-2-nonenal in cells. *Anal. Chem.* 87, 2535–2541.
- (29) Szychowski, J., Mahdavi, A., Hodas, J. J. L., Bagert, J. D., Ngo, J. T., Landgraf, P., Dieterich, D. C., Schuman, E. M., and Tirrell, D. A. (2010) Cleavable biotin probes for labeling of biomolecules via azide-alkyne cycloaddition. *J. Am. Chem. Soc.* 132, 18351–18360.
- (30) Boyce, M., Carrico, I. S., Ganguli, A. S., Yu, S.-H., Hangauer, M. J., Hubbard, S. C., Kohler, J. J., and Bertozzi, C. R. (2011) Metabolic cross-talk allows labeling of O-linked beta-N-acetylglucosamine-modified proteins via the N-acetylgalactosamine salvage pathway. *Proc. Natl. Acad. Sci. U. S. A.* 108, 3141–3146.
- (31) Qin, W., Qin, K., Fan, X., Peng, L., Hong, W., Zhu, Y., Lv, P., Du, Y., Huang, R., Han, M., Cheng, B., Liu, Y., Zhou, W., Wang, C., and Chen, X. (2018) Artificial Cysteine S-Glycosylation Induced by Per-O-Acetylated Unnatural Monosaccharides during Metabolic Glycan Labeling. *Angew. Chem., Int. Ed.* 57, 1817–1820.
- (32) Weerapana, E., Speers, A. E., and Cravatt, B. F. (2007) Tandem orthogonal proteolysis-activity-based protein profiling (TOP-ABPP)—a general method for mapping sites of probe modification in proteomes. *Nat. Protoc.* 2, 1414–1425.
- (33) Zhao, P., Viner, R., Teo, C. F., Boons, G.-J., Horn, D., and Wells, L. (2011) Combining high-energy C-trap dissociation and electron transfer dissociation for protein O-GlcNAc modification site assignment. *J. Proteome Res.* 10, 4088–4104.
- (34) Chalkley, R. J., and Burlingame, A. L. (2001) Identification of GlcNAcylation sites of peptides and  $\alpha$ -Crystallin using Q-TOF mass spectrometry. *J. Am. Soc. Mass Spectrom.* 12, 1106–1113.
- (35) Yang, J., Gupta, V., Tallman, K. A., Porter, N. A., Carroll, K. S., and Liebler, D. C. (2015) Global, in situ, site-specific analysis of protein S-sulfenylation. *Nat. Protoc.* 10, 1022–1037.
- (36) Schiapparelli, L. M., McClatchy, D. B., Liu, H.-H., Sharma, P., Yates, J. R., and Cline, H. T. (2014) Direct detection of biotinylated proteins by mass spectrometry. *J. Proteome Res.* 13, 3966–3978.
- (37) Rappsilber, J., Mann, M., and Ishihama, Y. (2007) Protocol for micro-purification, enrichment, pre-fractionation and storage of peptides for proteomics using StageTips. *Nat. Protoc.* 2, 1896–1906.
- (38) Ramakrishnan, B., and Qasba, P. K. (2002) Structure-based design of beta 1,4-galactosyltransferase I (beta 4Gal-T1) with equally efficient N-acetylgalactosaminyltransferase activity: point mutation broadens beta 4Gal-T1 donor specificity. *J. Biol. Chem.* 277, 20833–20839.
- (39) Clark, P. M., Dweck, J. F., Mason, D. E., Hart, C. R., Buck, S. B., Peters, E. C., Agnew, B. J., and Hsieh-Wilson, L. C. (2008) Direct in-gel fluorescence detection and cellular imaging of O-GlcNAc-modified proteins. *J. Am. Chem. Soc.* 130, 11576–11577.
- (40) Myers, S. A., Daou, S., Affar, E. B., and Burlingame, A. (2013) Electron transfer dissociation (ETD): the mass spectrometric breakthrough essential for O-GlcNAc protein site assignments—a study of the O-GlcNAcylated protein host cell factor C1. *Proteomics* 13, 982–991.
- (41) O’Shea, J. P., Chou, M. F., Quader, S. A., Ryan, J. K., Church, G. M., and Schwartz, D. (2013) pLogo: a probabilistic approach to visualizing sequence motifs. *Nat. Methods* 10, 1211–1212.
- (42) Levine, Z. G., Fan, C., Melicher, M. S., Orman, M., Benjamin, T., and Walker, S. (2018) O-GlcNAc Transferase Recognizes Protein Substrates Using an Asparagine Ladder in the Tetratricopeptide Repeat (TPR) Superhelix. *J. Am. Chem. Soc.* 140, 3510–3513.
- (43) Hu, C.-W., Worth, M., Fan, D., Li, B., Li, H., Lu, L., Zhong, X., Lin, Z., Wei, L., Ge, Y., Li, L., and Jiang, J. (2017) Electrophilic probes for deciphering substrate recognition by O-GlcNAc transferase. *Nat. Chem. Biol.* 13, 1267–1273.
- (44) Pathak, S., Alonso, J., Schimpl, M., Rafie, K., Blair, D. E., Borodkin, V. S., Schüttelkopf, A. W., Albarbarawi, O., and van Aalten, D. M. F. (2015) The active site of O-GlcNAc transferase imposes constraints on substrate sequence. *Nat. Struct. Mol. Biol.* 22, 744–750.
- (45) Lazarus, M. B., Nam, Y., Jiang, J., Sliz, P., and Walker, S. (2011) Structure of human O-GlcNAc transferase and its complex with a peptide substrate. *Nature* 469, 564–567.
- (46) Shen, D. L., Gloster, T. M., Yuzwa, S. A., and Vocadlo, D. J. (2012) Insights into O-linked N-acetylglucosamine ([O-9]O-GlcNAc) processing and dynamics through kinetic analysis of O-GlcNAc transferase and O-GlcNAcase activity on protein substrates. *J. Biol. Chem.* 287, 15395–15408.
- (47) Howerton, C. L., Morgan, C. P., Fischer, D. B., and Bale, T. L. (2013) O-GlcNAc transferase (OGT) as a placental biomarker of maternal stress and reprogramming of CNS gene transcription in development. *Proc. Natl. Acad. Sci. U. S. A.* 110, 5169–5174.
- (48) Pantaleon, M., Steane, S. E., McMahan, K., Cuffe, J. S. M., and Moritz, K. M. (2017) Placental O-GlcNAc-transferase expression and interactions with the glucocorticoid receptor are sex specific and regulated by maternal corticosterone exposure in mice. *Sci. Rep.* 7, 2017.
- (49) Howerton, C. L., and Bale, T. L. (2014) Targeted placental deletion of OGT recapitulates the prenatal stress phenotype including hypothalamic mitochondrial dysfunction. *Proc. Natl. Acad. Sci. U. S. A.* 111, 9639–9644.
- (50) Oishi, M., Gohma, H., Hashizume, K., Taniguchi, Y., Yasue, H., Takahashi, S., Yamada, T., and Sasaki, Y. (2006) Early embryonic death-associated changes in genome-wide gene expression profiles in the fetal placenta of the cow carrying somatic nuclear-derived cloned embryo. *Mol. Reprod. Dev.* 73, 404–409.
- (51) Grammel, M., and Hang, H. C. (2013) Chemical reporters for biological discovery. *Nat. Chem. Biol.* 9, 475–484.